

Innovative insertion material of $\text{LiAl}_{1/4}\text{Ni}_{3/4}\text{O}_2$ ($R\bar{3}m$) for lithium-ion (shuttlecock) batteries

Tsutomu Ohzuku *, Takayuki Yanagawa, Masaru Kouguchi, Atsushi Ueda

Electrochemistry and Inorganic Chemistry Laboratory, Department of Applied Chemistry, Faculty of Engineering, Osaka City University, Sugimoto 3-3-138, Sumiyoshi, Osaka 558, Japan

Accepted 27 December 1996

Abstract

We report an innovative insertion material of $\text{LiAl}_{1/4}\text{Ni}_{3/4}\text{O}_2$ ($R\bar{3}m$) which is a solid solution of LiNiO_2 ($R\bar{3}m$) and $\alpha\text{-LiAlO}_2$ ($R\bar{3}m$). $\text{LiAl}_{1/4}\text{Ni}_{3/4}\text{O}_2$ (interlayer distance: ~ 4.75 Å) shows an overcharge-resistant character due to the formation of an insulator of $\square_{3/4}\text{Li}_{1/4}\text{Al}_{1/4}\text{Ni}_{3/4}\text{O}_2$ having ~ 4.8 Å of interlayer distance. Cycle tests of an $\text{Li}/\text{LiAl}_{1/4}\text{Ni}_{3/4}\text{O}_2$ cell between 2.5 and 4.5 V show no noticeable loss in rechargeable capacity (~ 150 mAh g^{-1}). The thermal behavior of $\text{Li}_{1-x}\text{Al}_{1/4}\text{Ni}_{3/4}\text{O}_2$ ($0 \leq x < 3/4$) is also examined by differential scanning calorimetry and shows that the exothermic reaction of $\text{Li}_{1-x}\text{Al}_{1/4}\text{Ni}_{3/4}\text{O}_2$ with electrolyte is remarkably suppressed even for the fully charged state when compared with that of $\text{Li}_{1-x}\text{NiO}_2$. From these results we discuss on the possibility of designing reliable high-energy, high-volume, lithium-ion batteries. © 1997 Elsevier Science S.A.

Keywords: Lithium-ion batteries; Insertion materials

1. Introduction

Insertion materials for lithium-ion batteries, such as LiCoO_2 [1,2], $\text{LiCo}_{1/2}\text{Ni}_{1/2}\text{O}_2$ [3], LiNiO_2 [4,5] (or more generally $\text{LiCo}_x\text{Ni}_{1-x}\text{O}_2$ ($0 \leq x \leq 1$) [6–8]), LiMn_2O_4 [9–11] (or more generally $\text{Li}[\text{Li}_y\text{Mn}_{2-y}]\text{O}_4$ ($0 \leq y \leq 1/3$)) for positive electrode materials, and, carbon materials [12–14] or $\text{Li}[\text{Li}_{1/3}\text{Ti}_{5/3}]\text{O}_4$ [15,16] for negative electrode materials, have been investigated and some of them have already been used in practical lithium-ion batteries [17]. Of these, the combination of lithium nickelate and (natural) graphite is one of the most attractive systems for lithium-ion batteries. However, the results on failure mode analysis of lithium nickelate in lithium-ion batteries indicated that cycle-life failure, reactivity toward organic electrolyte oxidation, and so forth, were associated with the formation of nickel dioxide ($\square\text{NiO}_2$ ($R\bar{3}m$) [5]) which was metastable in nonaqueous environment at room temperature. In order to cope with the problems encountered in developing a lithium-ion battery consisting of LiNiO_2 and (natural) graphite, material design has been done in empirical, phenomenological basis in view of solid-state electrochemistry of insertion materials. The target material, $\text{LiAl}_{1/4}\text{Ni}_{3/4}\text{O}_2$, is a solid solution of LiNiO_2 ($R\bar{3}m$; $a = 2.88$ Å and $c = 14.19$ Å in hexagonal setting) and

$\alpha\text{-LiAlO}_2$ ($R\bar{3}m$; $a = 2.80$ Å and $c = 14.23$ Å [18]). In a previous paper [18] we have reported the effect of substitution of aluminum for nickel in LiNiO_2 upon the electrochemical properties.

In this paper we report on the cycle behavior of an $\text{Li}/\text{LiAl}_{1/4}\text{Ni}_{3/4}\text{O}_2$ cell in voltages between 2.5 and 4.5 V, the thermal behavior of $\text{Li}_{1-x}\text{Al}_{1/4}\text{Ni}_{3/4}\text{O}_2$ ($0 \leq x < 3/4$), and discuss whether or not reliable high-energy, high-volume, lithium-ion batteries are possible.

2. Experimental

$\text{LiAl}_{1/4}\text{Ni}_{3/4}\text{O}_2$ was prepared by heating a reaction mixture of LiNO_3 , NiCO_3 , and $\text{Al}(\text{OH})_3$ at 750 °C under an oxygen stream for 20 h [18]. The experimental cells and data acquisition system used in this study were the same as described in previous papers [19]. In examining the cycle behavior of an $\text{Li}/\text{LiAl}_{1/4}\text{Ni}_{3/4}\text{O}_2$ or Li/LiNiO_2 cell, the composition of electrode was 88 wt.% target sample, 6 wt.% acetylene black, and 6 wt.% Teflon binder (T-30J, Du Pont–Mitsui Fluorochemicals, Japan). Continuous charge and discharge tests in voltages between 2.5 and 4.5 V were done at 0.17 mA cm^{-2} . The electrolyte used was 1 M LiClO_4 dissolved in propylene carbonate (PC). For differential scanning calorimetric (DSC) study, partially or fully charged samples of $\text{LiAl}_{1/4}$

* Corresponding author.

$\text{Ni}_{3/4}\text{O}_2$ (or LiNiO_2) were prepared electrochemically using a compressed pellet of the sample without adding any conductive or organic binder (forming pressure: 10^3 kg cm^{-2} ; diameter: 11.3 mm, and thickness: $\sim 0.6 \text{ mm}$). The electrochemical oxidation of the pellets was performed galvanostatically at 0.2 mA cm^{-2} while monitoring the cell voltage. The degree of oxidation x in $\text{Li}_{1-x}\text{Al}_{1/4}\text{Ni}_{3/4}\text{O}_2$ (or in $\text{Li}_{1-x}\text{NiO}_2$) was calculated from the charge capacity and the theoretical capacity based on a one-electron transfer per $\text{LiAl}_{1/4}\text{Ni}_{3/4}\text{O}_2$ (299 mAh g^{-1}) or LiNiO_2 (275 mAh g^{-1}). The sample (20–30 mg) containing the electrolyte was sealed in an aluminum cell (diameter: 5.5 mm, thickness: $\sim 1 \text{ mm}$). Twenty mg of $\alpha\text{-Al}_2\text{O}_3$ in the aluminum cell was used as a reference. All procedures for handling and fabricating the electrochemical cells were performed in an argon-filled glove box. The other sets of experimental conditions are given in Section 3.

3. Results and discussion

Figs. 1 and 2 show continuous charge and discharge curves of an Li/LiNiO_2 and $\text{Li}/\text{LiAl}_{1/4}\text{Ni}_{3/4}\text{O}_2$ cell, respectively. These cells were operated in voltages between 2.5 and 4.5 V at a rate of 0.17 mA cm^{-2} (0.5 mA per 3 cm^2 of apparent electrode area) at 30°C . The capacities in the figures are given in mAh g^{-1} based on the sample weight. As can be seen in Fig. 1, an Li/LiNiO_2 cell deteriorates so rapidly when it operates between 2.5 and 4.5 V, while the cell can operate without any noticeable loss in rechargeable capacity for such a limited cycle test with charge-end voltage below 4.2 V (typically 4.1 V) [5,20]. Such a cycle-life failure is due to the formation of nickel dioxide at voltages above 4.2 V versus lithium [5]. During the oxidation of LiNiO_2 the interlayer distance between NiO_2 sheets expands almost continuously from ~ 4.73 to $\sim 4.8 \text{ \AA}$ as x in $\text{Li}_{1-x}\text{NiO}_2$ approaches 0.5

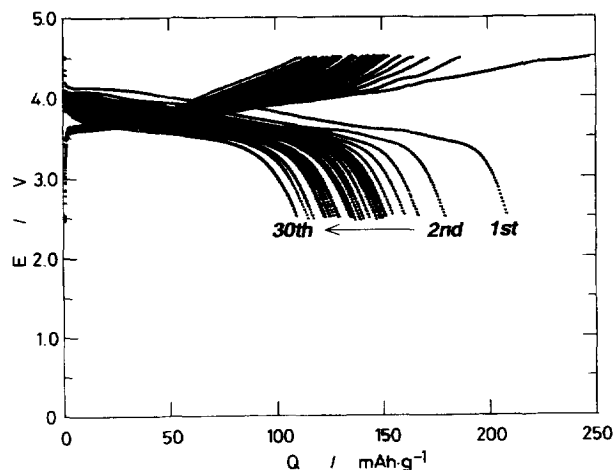


Fig. 1. Charge and discharge curves of an Li/LiNiO_2 cell operated in voltages between 2.5 and 4.5 V at 30°C . The current applied was 0.5 mA per 3 cm^2 (0.17 mA cm^{-2}) for both the positive and the negative electrodes. Electrolyte used was 1 M LiClO_4 dissolved in PC. LiNiO_2 loaded on positive electrode was 86.8 mg .

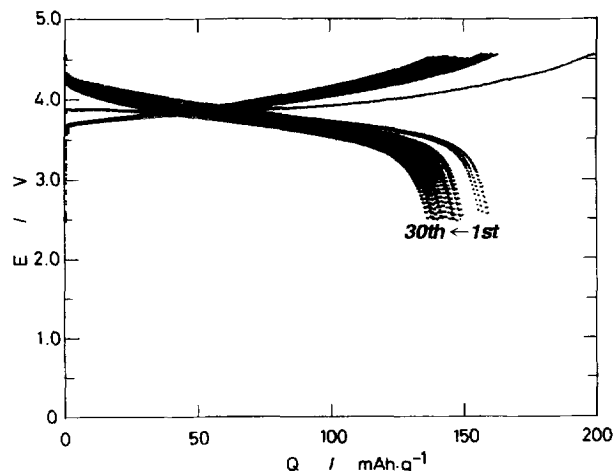


Fig. 2. Charge and discharge curves of an $\text{Li}/\text{LiAl}_{1/4}\text{Ni}_{3/4}\text{O}_2$ cell operated in voltages between 2.5 and 4.5 V at 30°C . The current applied was 0.5 mA per 3 cm^2 (0.17 mA cm^{-2}) for both the positive and the negative electrode. $\text{LiAl}_{1/4}\text{Ni}_{3/4}\text{O}_2$ loaded on positive electrode was 101.9 mg .

and then it leveled off until 0.75. Rechargeability is excellent in this region because of mild change in interlayer distance. However, further oxidation above 0.75 results in sudden change in interlayer distance down to $\sim 4.5 \text{ \AA}$ during which the open-circuit voltage stays at $\sim 4.2 \text{ V}$. The rigorous limitation concerning the charge-end voltage below 4.2 V versus lithium makes it difficult to use LiNiO_2 for lithium-ion batteries, because such an exact voltage regulation of the positive electrode cannot be done in lithium-ion batteries unless auxiliary a lithium electrode is properly placed.

An $\text{Li}/\text{LiAl}_{1/4}\text{Ni}_{3/4}\text{O}_2$ cell shows better capacity retention than an Li/LiNiO_2 cell as was shown in Fig. 2. However, rechargeable capacity seems to fade cycle by cycle. In order to examine whether or not capacity fading is derived from the destruction of $\text{LiAl}_{1/4}\text{Ni}_{3/4}\text{O}_2$ structure, the cell was charged at constant voltage of 4.5 V for 12 h following constant-current charge at 0.17 mA cm^{-2} after the 31st discharge. Results are shown in Fig. 3. After the constant-voltage charge at 4.5 V, capacity is recovered at such a degree that the cell delivered at the sixth discharge, see Fig. 2. As clearly be seen in Fig. 3, $\text{LiAl}_{1/4}\text{Ni}_{3/4}\text{O}_2$ is capable of constant-voltage charging at 4.5 V. Although increase in polarization for both charging and discharging is seen in Fig. 3, we confirm a superior character of $\text{LiAl}_{1/4}\text{Ni}_{3/4}\text{O}_2$ in applying this material to lithium-ion batteries. Fig. 4 shows the X-ray diffraction (XRD) pattern of the positive electrode experienced 32 charge and discharge cycles. The XRD examination was done in a discharge state. The starting sample of $\text{LiAl}_{1/4}\text{Ni}_{3/4}\text{O}_2$ is also shown by comparison. In measuring the XRD pattern of $\text{LiAl}_{1/4}\text{Ni}_{3/4}\text{O}_2$, an aluminum holder for powdered sample was used, so that comparison in intensity between two XRD data cannot be done in this case. As can be seen in Fig. 4, no additional diffraction line, even line broadening of each diffraction line cannot be found, indicating that the core structure of $\text{LiAl}_{1/4}\text{Ni}_{3/4}\text{O}_2$ is not damaged during charge and discharge between 2.5 and 4.5 V because the fully charged state

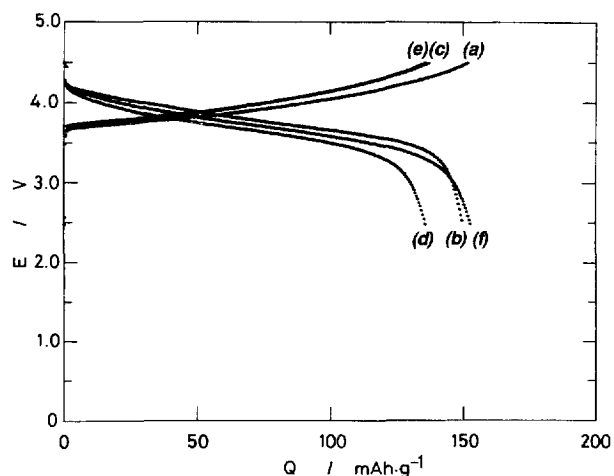


Fig. 3. Effect of constant-voltage charge at 4.5 V following constant-current charge to 4.5 V upon rechargeable capacity of a Li/LiAl_{1/4}Ni_{3/4}O₂ cell: (a) the 6th charge; (b) 6th discharge; (c) 31st charge; (d) 31st discharge; (e) 32nd charge, and (f) 32nd discharge. After the 31st discharge, the cell was charged at 0.17 mA cm⁻² to 4.5 V and then kept at constant voltage of 4.5 V for 12 h. The capacity was recovered by constant-voltage charging at 4.5 V, which cannot be attained for an Li/LiNiO₂ or LiCoO₂ cell.

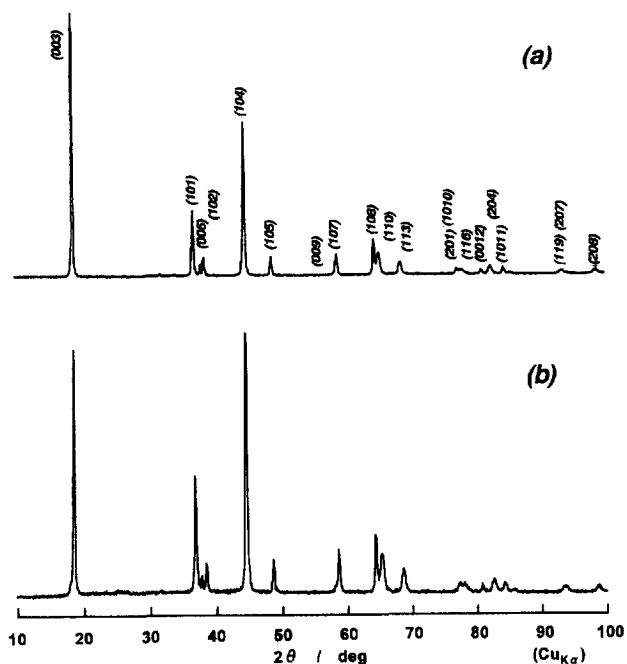


Fig. 4. The XRD pattern of the LiAl_{1/4}Ni_{3/4}O₂ electrode after 32 cycles in voltages between 2.5 and 4.5 (shown in (b)). Starting material of LiAl_{1/4}Ni_{3/4}O₂ is also shown in (a) for comparison.

of this material is $\square_{3/4}\text{Li}_{1/4}\text{Al}_{1/4}\text{Ni}_{3/4}\text{O}_2$ having ~ 4.8 Å of interlayer distance [18].

Thermal behavior on partially or fully charged state of insertion materials with electrolyte is another factor associated with safety in considering positive electrodes for lithium-ion batteries. Fig. 5 shows results on the DSC measurements of the Li_{1-x}NiO₂ ($0 \leq x < 1$) prepared by the electrochemical oxidation of LiNiO₂, LiNiO₂ and $\square_{1/4}\text{Li}_{3/4}\text{NiO}_2$ are stable even when they are heated with an organic electrolyte as shown in Fig. 5. $\square_{1/2}\text{Li}_{1/2}\text{NiO}_2$ shows some exothermic

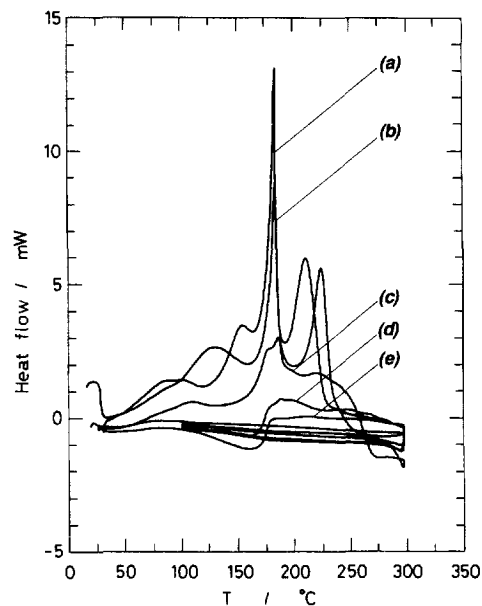


Fig. 5. DSC curves for (a) $\square_{0.85}\text{Li}_{0.15}\text{NiO}_2$ (23.2 mg), (b) $\square_{3/4}\text{Li}_{1/4}\text{NiO}_2$ (23.5 mg), (c) $\square_{1/2}\text{Li}_{1/2}\text{NiO}_2$ (16.6 mg), (d) $\square_{1/4}\text{Li}_{3/4}\text{NiO}_2$ (22.6 mg), and (e) LiNiO₂ (24.1 mg). The weight in parentheses contains the electrolyte. A heating and cooling rate was 5 °C min⁻¹.

peaks around 180 °C, but it seems to be mild in this stage. An endothermic signal in temperatures between 100 and 180 °C is due to the decomposition of PC. However, when $\square_{3/4}\text{Li}_{1/4}\text{Ni}_{3/4}\text{O}_2$ or $\square_{0.85}\text{Li}_{0.15}\text{NiO}_2$ (fully charged state of LiNiO₂ under this experimental condition) is heated at a rate of 5 °C min⁻¹, exothermic DSC signals of heat flow in mW were observed until the decomposition reaction of the sample completed at about 250 °C. The exothermic signals increase as temperature rises and then rapidly increase at about 160 °C drawing a spike at 185 °C. Rapid increase and decrease drawing a spike in DSC signals at 185 °C consist of an electrolyte oxidation (exothermic) and a decomposition (endothermic) reaction of $\square_{3/4}\text{Li}_{1/4}\text{NiO}_2$ or $\square_{0.85}\text{Li}_{0.15}\text{NiO}_2$ releasing oxygen, whose onset temperature is 185 °C, confirmed by thermogravimetry and XRD. The product was identified as nickel monoxide (NiO). Although the decomposition reaction releasing oxygen is an endothermic reaction, it turns out to be an exothermic reaction as a whole, if oxygen meets reducing agents, such as lithiated (high-area) carbons.

While the onset temperature of an exothermic spike in Fig. 5 is ~ 160 °C, the exothermic heat flow almost continuously increases as temperature rises from room temperature. This strongly suggests that an exothermic reaction proceeds even at room temperature and the reaction rate is accelerated as temperature rises. Such a thermal behavior of Li_{1-x}NiO₂ ($1/2 < x < 1$) in Fig. 5 reminds us a 'hay-stack' or 'clock' reaction associated with thermal runaway. When an exothermic reaction proceeds in a reaction vessel, temperature continuously rises unless the rate of heat generation due to chemical reactions is less than that of heat escape from the surface of a vessel. The reaction rate is usually accelerated as temperature rises by self-heating due to an exothermic reac-

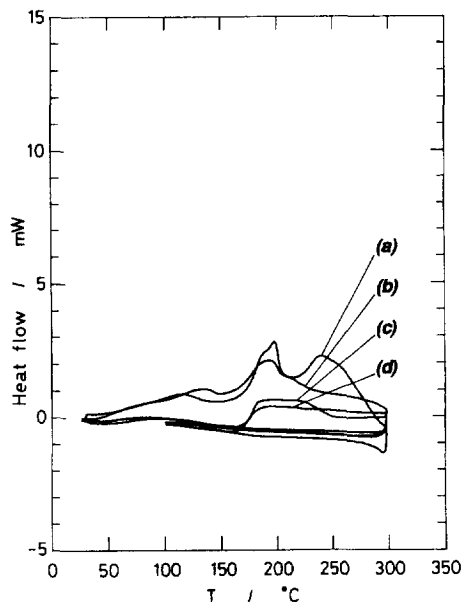


Fig. 6. DSC curves for (a) $\square_{0.69}\text{Li}_{0.31}\text{Al}_{1/4}\text{Ni}_{3/4}\text{O}_2$ (20.5 mg), (b) $\square_{1/2}\text{Li}_{1/2}\text{Al}_{1/4}\text{Ni}_{3/4}\text{O}_2$ (20.5 mg), (c) $\square_{1/4}\text{Li}_{3/4}\text{Al}_{1/4}\text{Ni}_{3/4}\text{O}_2$ (20.1 mg), and (d) $\text{LiAl}_{1/4}\text{Ni}_{3/4}\text{O}_2$ (20.9 mg). The weight in parentheses contains electrolyte. A heating and cooling rate was 5°C min^{-1} .

tion and eventually the evolution of temperature leads to thermal runaway. Such a delayed action about thermal runaway makes it difficult to predict or forewarn about when thermal runaway takes place, i.e., one cannot tell one day, one week, or one year after a clock reaction is switched on in a reaction vessel. This is the reason that LiNiO_2 is difficult to be applied to lithium-ion batteries in spite of its higher rechargeable capacity than LiCoO_2 .

Fig. 6 shows the DSC results on $\text{Li}_{1-x}\text{Al}_{1/4}\text{Ni}_{3/4}\text{O}_2$ containing electrolyte. As can be seen in Fig. 6, exothermic reactions are remarkably suppressed by substituting aluminum for nickel in LiNiO_2 while retaining high-voltage, high-capacity characteristic of lithium nickelate as was shown in Fig. 2. Noticeable exothermic peak cannot be seen even for a fully charged state of $\text{LiAl}_{1/4}\text{Ni}_{3/4}\text{O}_2$ ($\square_{0.69}\text{Li}_{0.31}\text{Al}_{1/4}\text{Ni}_{3/4}\text{O}_2$ in this case). Such a thermal behavior of $\text{Li}_{1-x}\text{Al}_{1/4}\text{Ni}_{3/4}\text{O}_2$ will not lead to thermal runaway as was described above.

Although $\text{LiAl}_{1/4}\text{Ni}_{3/4}\text{O}_2$ has a slightly larger polarization character than LiCoO_2 , LiNiO_2 , or $\text{LiCo}_{1/4}\text{Ni}_{3/4}\text{O}_2$ [1,8] with rechargeable capacity of about 150 mAh g^{-1} based on $\text{LiAl}_{1/4}\text{Ni}_{3/4}\text{O}_2$ weight, we are expecting 200 mAh g^{-1} of rechargeable capacity out of 224 mAh g^{-1} of a theoretical capacity with smaller polarization than for LiCoO_2 or

$\text{LiCo}_{1/4}\text{Ni}_{3/4}\text{O}_2$ by improving the processing methods to prepare the samples and electrodes. Such approaches are under way in our laboratory. We believe that the combination of $\text{LiAl}_{1/4}\text{Ni}_{3/4}\text{O}_2$ ($R\bar{3}m$) and (natural) graphite is a most attractive system for reliable high-energy, high-volume, lithium-ion batteries.

Acknowledgements

The present work was partly supported by a grant-in-aid for Scientific Research from the Ministry of Education, Science and Culture, Japan.

References

- [1] K. Mizushima, P.C. Jones, P.J. Wiseman and J.B. Goodenough, *Mater. Res. Bull.*, 15 (1980) 783.
- [2] T. Ohzuku and A. Ueda, *J. Electrochem. Soc.*, 141 (1994) 2972.
- [3] A. Ueda and T. Ohzuku, *J. Electrochem. Soc.*, 141 (1994) 2013.
- [4] J.R. Dahn, U. von Sacken, M.W. Juzkow and H. Al-Janaby, *J. Electrochem. Soc.*, 138 (1991) 2207.
- [5] T. Ohzuku, A. Ueda and M. Nagayama, *J. Electrochem. Soc.*, 140 (1993) 1862.
- [6] T. Ohzuku, H. Komori, K. Sawai and T. Hirai, *Chem. Express*, 5 (1990) 733.
- [7] C. Delmas and I. Saadoune, *Solid State Ionics*, 53–56 (1992) 370.
- [8] T. Ohzuku, A. Ueda, M. Nagayama, Y. Iwakoshi and H. Komori, *Electrochim. Acta*, 38 (1993) 1159.
- [9] W.I.F. David, M.M. Thackeray, P.G. Bruce and J.B. Goodenough, *Mater. Res. Bull.*, 19 (1984) 99.
- [10] T. Ohzuku, M. Kitagawa and T. Hirai, *J. Electrochem. Soc.*, 137 (1990) 769.
- [11] J.M. Tarascon, D. Guyomard and G.L. Baker, *J. Power Sources*, 43–44 (1993) 689.
- [12] T. Ohzuku, Y. Iwakoshi and K. Sawai, *J. Electrochem. Soc.*, 140 (1993) 2494.
- [13] J.R. Dahn, A.K. Sleight, H. Shi, B.M. Way, W.J. Weydanz, J.N. Reimers, Q. Zhong and U. von Sacken, in G. Pistoia (ed.), *Lithium Batteries*, Elsevier, Amsterdam, 1993, Ch. 1.
- [14] K. Sawai, Y. Iwakoshi and T. Ohzuku, *Solid State Ionics*, 69 (1994) 273.
- [15] T. Ohzuku, A. Ueda and N. Yamamoto, *J. Electrochem. Soc.*, 142 (1995) 1431.
- [16] T. Ohzuku, A. Ueda, N. Yamamoto and Y. Iwakoshi, *J. Power Sources*, 54 (1995) 99.
- [17] T. Ohzuku and A. Ueda, *Solid State Ionics*, 69 (1994) 201.
- [18] T. Ohzuku, A. Ueda and M. Kouguchi, *J. Electrochem. Soc.*, 142 (1995) 4033.
- [19] T. Ohzuku, M. Kitagawa and T. Hirai, *J. Electrochem. Soc.*, 136 (1989) 3169; 137 (1990) 40.
- [20] M. Broussely, F. Pertion, P. Biensan, J.M. Bodet, J. Labat, A. Lecerf, C. Delmas, A. Rougier and J.P. Peres, *J. Power Sources*, 54 (1995) 109.